Optimal Symmetric Flight with an Intermediate Vehicle Model

P.K.A. Menon,* H.J. Kelley,† and E.M. Cliff‡
Virginia Polytechnic Institute and State University, Blacksburg, Virginia

Optimal flight in the vertical plane with a vehicle model intermediate in complexity between point-mass and energy models is studied. Flight-path angle takes on the role of a control variable. The class of altitude-speed-range-time optimization problems with fuel expenditure unspecified is investigated and some interesting phenomena uncovered. The maximum-lift-to-drag glide appears as part of the family, final-time-open, with appropriate initial and terminal transient maneuvers. A family of climb-range paths appears for thrust exceeding level-flight drag, some members exhibiting oscillations. Oscillatory paths generally fail the Jacobi test for durations exceeding a period and furnish a minimum only for short-duration problems.

Introduction

THERE has been interest from the beginning of optimal-flight studies in approximations featuring simplified vehicle models. Representation of drag as the drag for level flight leads to an intermediate vehicle model in which path angle γ takes on the role of a control variable and the order of the system is reduced by one. An additional order reduction leads to an "energy-state" model with altitude or speed as a control variable.[1-3] This is reviewed in a companion paper.[4] The present paper examines optimal symmetric flight with the intermediate vehicle model.

The analysis is based in part upon an exploration of Euler solutions for the path-angle-as-control model carried out in Ref. 5. The present analysis examines higher-order optimality conditions and "chattering control" phenomena. The weakness of the model will be seen as more extensive than previously noted.

Intermediate Vehicle Model

The point-mass dynamical model of aircraft flight incorporating the assumption of thrust-along-the-path is given by

$$\dot{V}=g\left[\frac{T-D}{W}-\sin\gamma\right] \tag{1}$$

$$\dot{h}=V\sin\gamma \tag{2}$$

$$\dot{x}=V\cos\gamma \tag{3}$$

$$\dot{\tilde{W}}=Q \tag{4}$$

$$\dot{\gamma}=\frac{g}{V}\left(\frac{L}{W}-\cos\gamma\right) \tag{5}$$

where V is airspeed, h altitude, x down-range, W aircraft weight, $\tilde{W}$ weight of fuel consumed, γ flight-path angle, T thrust, D drag, g the acceleration due to gravity, L lift, and Q the fuel-consumption rate.

The sweeping assumption that drag can be approximated by its level-flight value is next invoked. This permits the deletion of Eq. (5) and the elevation of path-angle γ to control status. Lift coefficient, C_L, or angle of attack, α, previously a control variable, is correspondingly assumed to be such as to satisfy Eq. (5). There is obviously trouble ahead with this modeling should $\dot{\gamma}$ turn out to be large in optimized maneuvering or, worse yet, should γ exhibit jump behavior.

The optimal-control problem to be treated, then, is the minimization of a function of the final values of the state variables and final time.

The Hamiltonian function is

$$H=\lambda_V g\left\{\frac{(T-D)}{W}-\sin\gamma\right\}+\lambda_h V\sin\gamma+\lambda_x V\cos\gamma+\lambda_{\tilde{W}}Q \tag{6}$$

and the Euler-Lagrange equations are

$$\dot{\lambda}_V=-\lambda_V\frac{q}{W}\frac{\partial}{\partial V}(T-D)-\lambda_h\sin\gamma-\lambda_x\cos\gamma-\lambda_{\tilde{W}}\frac{\partial Q}{\partial V} \tag{7}$$

$$\dot{\lambda}_h=-\lambda_V\frac{g}{W}\frac{\partial}{\partial h}(T-D)-\lambda_{\tilde{W}}\frac{\partial Q}{\partial h} \tag{8}$$

$$\dot{\lambda}_x=0 \tag{9}$$

$$\dot{\lambda}_{\tilde{W}}=0 \tag{10}$$

and

$$-\lambda_V g\cos\gamma+\lambda_h V\cos\gamma-\lambda_x V\sin\gamma=0 \tag{11}$$

In the following, the time derivatives of Eq. (11) will be used to eliminate the time-varying costates in favor of the control γ and derivatives. Note that this is somewhat formal since $\dot{\gamma}$ may not exist. Using Eq. (7-11) those costates which are variable in the Hamiltonian may now be eliminated. Using Eq. (11)

$$\lambda_V=\frac{V}{g}(\lambda_h-\lambda_x\tan\gamma) \tag{12}$$

and hence

$$\dot{\lambda}_V=\frac{\dot{V}}{g}(\lambda_h-\lambda_x\tan\gamma)+\frac{V}{g}(\dot{\lambda}_h-\lambda_x\dot{\gamma}\sec^2\gamma) \tag{13}$$

Substituting for λ_V from Eq. (12) in Eq. (8),

$$\dot{\lambda}_h+\frac{V}{W}(\lambda_h-\lambda_x\tan\gamma)\frac{\partial}{\partial h}(T-D)+\lambda_{\tilde{W}}\frac{\partial Q}{\partial h}=0 \tag{14}$$

Submitted July 11, 1983; presented as Paper 83-2238 at the AIAA Guidance and Control Conference, Gatlinburg, Tenn., Aug. 15-17, 1983; revision submitted June 20, 1984.

*Presently with Integrated Systems Inc., Palo Alto, California.

Using Eq. (13) in Eq. (7) and using Eqs. (1) and (12), a second expression for $\dot{\lambda}_h$ as

$$\dot{\lambda}_h+\lambda_h\frac{g}{W}\left[\frac{(T-D)}{V}+\frac{\partial}{\partial V}(T-D)\right]+\lambda_x\left[\frac{g}{V\cos\gamma}-\dot{\gamma}\sec^2\gamma\right.$$
$$\left.-\frac{g}{W}\tan\gamma\left\{\frac{(T-D)}{V}+\frac{\partial}{\partial V}(T-D)\right\}\right]+\lambda_{\tilde{w}}\frac{g}{V}\frac{\partial Q}{\partial V}=0 \quad (15)$$

Equations (14) and (15) may now be used to obtain an expression for λ_h in terms of λ_x and $\lambda_{\tilde{w}}$.

$$\frac{\lambda_h}{W}\left[\frac{\partial}{\partial h}V(T-D)-\frac{g}{V}\frac{\partial}{\partial V}V(T-D)\right]$$
$$-\lambda_x\left[\tan\gamma\left\{\frac{\partial}{\partial h}V(T-D)-\frac{g}{V}\frac{\partial}{\partial V}V(T-D)\right\}\right.$$
$$\left.+\frac{g}{V\cos\gamma}-\dot{\gamma}\sec^2\gamma\right]+\lambda_{\tilde{w}}\left[\frac{\partial Q}{\partial h}-\frac{g}{V}\frac{\partial Q}{\partial V}\right]=0 \quad (16)$$

Expressions (12) and (16) may be used for eliminating λ_V and λ_h in the Hamiltonian with the following result:

$$\cos\gamma H\left\{\left[\frac{\partial}{\partial h}-\frac{g}{V}\frac{\partial}{\partial V}\right]\left(V(T-D)\right)\right\}$$
$$-\cos\gamma\lambda_{\tilde{w}}Q^2\left\{\left[\frac{\partial}{\partial h}-\frac{g}{V}\frac{\partial}{\partial V}\right]\left(\frac{V(T-D)}{Q}\right)\right\}$$
$$-\lambda_x\left\{V^2\left[\frac{\partial}{\partial h}-\frac{g}{V}\frac{\partial}{\partial V}\right]\left(\frac{(T-D)}{}\right)-\frac{(T-D)V}{\cos\gamma}\dot{\gamma}\right\}=0 \quad (17)$$

Note that

$$\left\{\frac{\partial}{\partial h}-\frac{g}{V}\frac{\partial}{\partial V}\right\}[\ ]=\frac{\partial}{\partial h}[\ ]\Big|_{E=\text{const}}$$

where $E=h+V^2/2g$, the specific energy.

In order to investigate the implications of this complicated expression, consider first the case of free final value of range x and *fuel* $\tilde{W}$. If the final values of these variables are left open, then the natural boundary conditions $\lambda_x=0$ and $\lambda_{\tilde{W}}=0$ apply and the optimization problem is a tradeoff between final values of time t, altitude h, and airspeed V, the maximum or minimum value of one of these variables, or some function of these variables being sought without regard to range or fuel consumption. In Eq. (17), if the transversality condition for minimum time, $H=-1$, is imposed, the well known energy-climb schedule is obtained.

Note that in this case, Eq. (17) can be satisfied either by $\cos\gamma=0$, vertical flight, or by vanishing of the bracketed expression, viz., the partial derivative of specific excess power $V(T-D)$ with respect to altitude with specific energy held constant. Thus, the solution of this or any *h-V-t* optimum problem is made up of vertical climbs, vertical dives, and "energy climbs" pieced together in the proper order. Similar considerations apply if fuel expenditure rather than time is to be minimized. In this case $H=0$, $\lambda_x=0$ and $\lambda_{\tilde{W}}=1$, and Eq. (17) yields the minimum-fuel climb path with fixed throttle in the *V-h* plane.

If range is to be maximized or minimized with final time and fuel unspecified, then $\lambda_x=\mp1$ and $H=\lambda_{\tilde{W}}=0$, and a first-order differential equation for path inclination emerges as follows:

$$\left\{V^2\left[\frac{\partial}{\partial h}-\frac{g}{V}\frac{\partial}{\partial V}\right](T-D)-\frac{(T-D)V\dot{\gamma}}{\cos\gamma}\right\}=0 \quad (18)$$

If $\lambda_x=-1$ and a fixed value of H (to be determined) with $\lambda_{\tilde{W}}=0$ are chosen, Eq. (17) is the Euler equation for maximizing range-to-climb with fixed final time. With $H=0$, $\lambda_x=-1$ and a fixed value of $\lambda_{\tilde{W}}$, similarly the maximum range to climb trajectory with fixed final value of fuel is obtained. It may be noted that the maximum-range-to-climb problem is ill-posed in that the range-to-climb for thrust greater than drag without time or fuel constraints does not have a maximum, or even an upper-bound. Further, fixed-throttle, range-fuel trajectories are not of significant interest in practical situations. Hence, attention will be focused on the problem of maximizing the range-to-climb with a specified final time (fixed $H\neq0$, $\lambda_x=-1$).

The system of Eqs. (1-3) and (18) generates a trajectory family for the range problem. The possibility of obtaining an analytical solution of the system for the case of thrust and drag as arbitrary functions of altitude and air speed is remote. However, using the assumption of constant-density atmosphere, with thrust and drag dependent on airpseed only, one can obtain an analytical solution to this system.[5] Equation (18) can be rewritten as

$$\frac{\dot{\gamma}}{\cos\gamma}=\frac{V}{(T-D)}\left\{\frac{\partial}{\partial h}-\frac{g}{V}\frac{\partial}{\partial V}\right\}(T-D) \quad (19)$$

In the following, several transformations of independent variable are carried out without attention to monotonicity requirements, the thought being to fit the solution segments obtained into families in due course. The temptation of range as independent variable will be avoided, however, in anticipation of purely-vertical-motion segments. In the interest of breavity we designate $\mu\equiv(T-D)/W$, so that

$$\frac{1}{\cos\gamma}\frac{\mathrm{d}\gamma}{\mathrm{d}V}(\sin\gamma+\mu)=\frac{V}{g\mu}\left\{\frac{\partial}{\partial h}-\frac{g}{V}\frac{\partial}{\partial V}\right\}\mu \quad (20)$$

With altitude-dependence suppressed, the path angle γ is determined as the solution of the first-order differential equation

$$\frac{1}{\cos\gamma}\frac{\mathrm{d}\gamma}{\mathrm{d}V}(\sin\gamma-\mu)=\frac{\mathrm{d}\mu}{\mathrm{d}V}\frac{1}{\mu} \quad (21)$$

Further simplification is obtained by another change of independent variable, this time from V to μ

$$\frac{1}{\cos\gamma}\frac{\mathrm{d}\gamma}{\mathrm{d}\mu}(\sin\gamma-\mu)=\frac{1}{\mu} \quad (22)$$

If the roles of independent and dependent variables are now regarded as reversed, this equation takes the form

$$\frac{\mathrm{d}\mu}{\mathrm{d}\gamma}+\frac{1}{\cos\gamma}\mu^2-\mu\frac{\sin\gamma}{\cos\gamma}=0 \quad (23)$$

which is the form of the Bernoulli differential equation. According to Kamke,[6] this equation has the solution

$$\frac{1}{\mu}=\sin\gamma+C\cos\gamma \quad (24)$$

Before expressing this relationship in the form $\gamma=\gamma(\mu)$, we relate the integration constant C to equilibrium values of μ and γ corresponding to unaccelerated flight. Such values may be designated with a superscribed bar:

$$\bar{\mu}=\sin\bar{\gamma} \quad (25)$$

$$C=\cot\bar{\gamma} \quad (26)$$

The solution may then be expressed as:

$$\gamma = \tilde{\gamma} + \cos^{-1}\left[\frac{\tilde{\mu}}{\mu}\right] \tag{27}$$

Here $\tilde{\mu}$ is the value of μ in unaccelerated flight and

$$\tilde{\gamma} = \sin^{-1}\tilde{\mu} \tag{28}$$

In Fig. 1, the solution (27) is illustrated for various values of $\tilde{\mu}$. The range of angle γ has been restricted to ± 180 deg in this plot.

With this solution at hand, the state histories can be generated. If the thrust is taken as zero, the state-Euler system produces the flattest glide trajectory, flown with maximum lift-to-drag ratio, along with a family of transients to and from this point (Fig. 2). When a positive margin of thrust over drag exists, a family of oscillatory solutions is generated for various values of $\tilde{\mu}$ as shown in Fig. 3. It may be noted in Fig. 3 that the innermost point corresponding to $\mu = 0.2$ in $V-\gamma$ space corresponds to flight at $(T-D)_{\max}$, while along the outermost closed path, the flight path angle γ switches between $\pm$ 90 deg.

With the availability of the Euler solution (27) to the maximum-range problem with altitude dependence suppressed, similar solution to the more general Euler equation (17) may be obtained using variation of parameters.[7] Equation (17) may be written as

$$\dot{\gamma} = -g\left\{\frac{\cos\gamma}{\mu}\frac{\partial\mu}{\partial V} - \cos^2\gamma\frac{H}{\lambda_x}\frac{1}{V^2\mu}\frac{\partial}{\partial V}(V\mu) + \cos^2\gamma\frac{\lambda_{\tilde{W}}}{\lambda_x}\frac{Q^2}{V^2\mu}\frac{\partial}{\partial V}\left[\frac{V\mu}{Q}\right]\right\} \tag{29}$$

As in Eq. (21), the independent variable is changed from time to airspeed resulting in

$$\frac{d\gamma}{dV}(\sin\gamma - \mu) = \frac{\cos\gamma}{\mu}\frac{d\mu}{dV} - \cos^2\gamma\frac{H}{\lambda_x}\frac{1}{V^2\mu}\frac{d}{dV}(V\mu) + \cos^2\gamma\frac{\lambda_{\tilde{W}}}{\lambda_x}\frac{Q^2}{V^2\mu}\frac{d}{dV}\left[\frac{V\mu}{Q}\right] \tag{30}$$

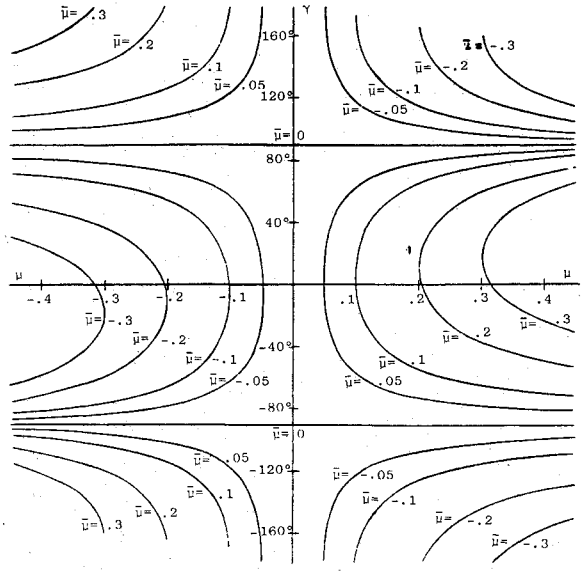

Fig. 1 Flight-path angle vs acceleration variable for the range problem.

Expression (24) may be differentiated with respect to airspeed to obtain

$$-\frac{1}{\mu^2}\frac{d\mu}{dV} = (\cos\gamma - C\sin\gamma)\frac{d\gamma}{dV} + \frac{dC}{dV}\cos\gamma \tag{31}$$

Note that C is no longer a constant here, but a function of the independent variable V. Substituting for μ in Eq. (31) from Eq. (24)

$$\frac{1}{\mu}\frac{d\mu}{dV} = -\frac{\left[(\cos\gamma - C\sin\gamma)\frac{d\gamma}{dV} + \frac{dC}{dV}\cos\gamma\right]}{(\sin\gamma + C\cos\gamma)} \tag{32}$$

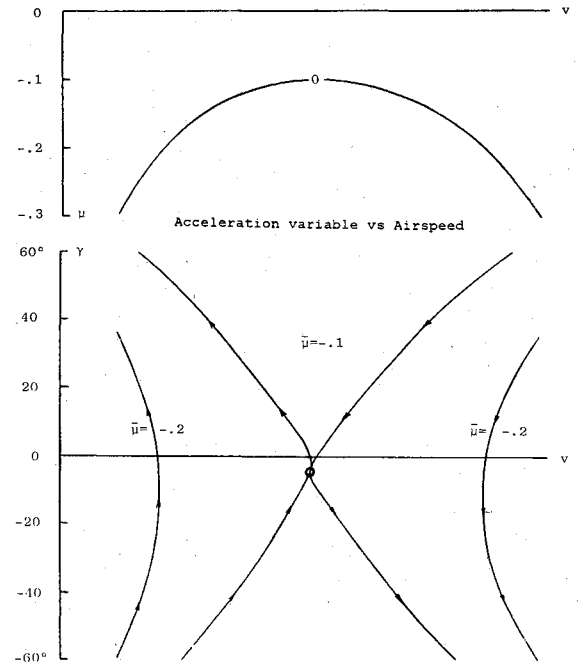

Fig. 2 Flight-path angle vs airspeed in gliding flight for the range problem.

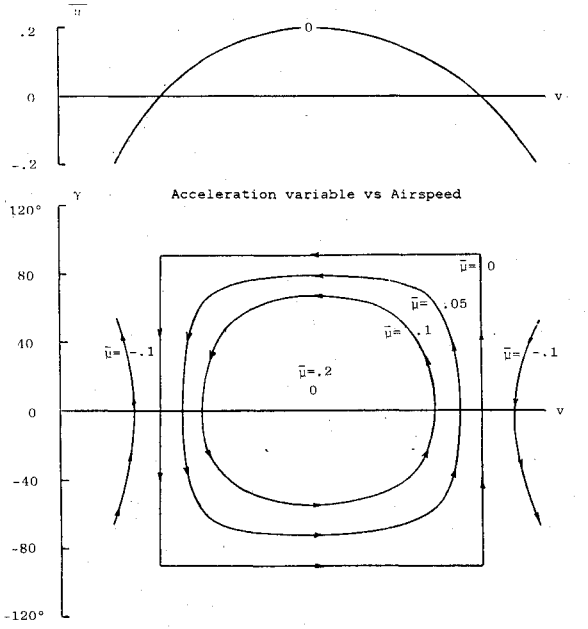

Fig. 3 Flight-path angle vs airspeed in powered flight for the range problem.

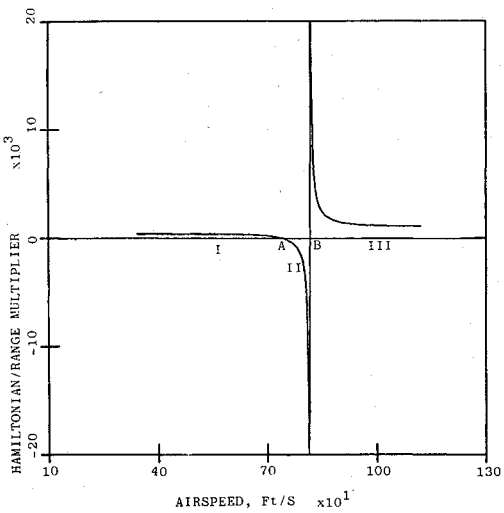

Fig. 4 H/λ_x vs airspeed for equilibrium flight (parabolic $(T-D)/W$ distribution), A) $(T-D)_{max}$; B) $V(T-D)_{max}$.

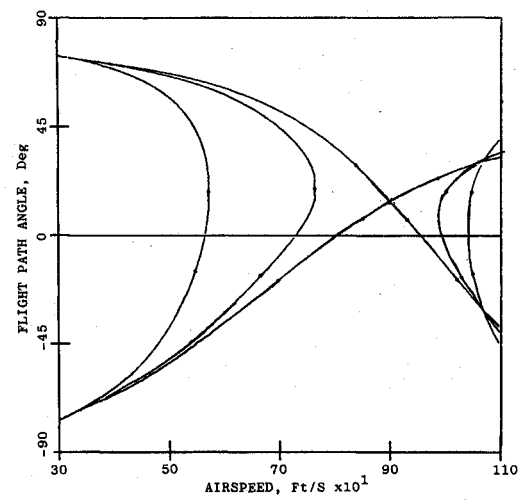

Fig. 5 Representative analytical solution for H/λ_x in the third equilibrium regime.

Using Eq. (32) in Eq. (30) and since $\mu = 1/\sin\gamma + C\cos\gamma$ from Eq. (24),

$$\cos^2\gamma \frac{dC}{dV} = \cos^2\gamma\left[-\frac{H}{\lambda_x}\left\{\frac{1}{V^2\mu} + \frac{1}{V\mu^2}\frac{d\mu}{dV}\right\} + \frac{\lambda_{\tilde{W}}}{\lambda_x}\left\{\frac{Q}{V^2\mu} + \frac{Q}{V\mu^2}\frac{d\mu}{dV} - \frac{1}{V\mu}\frac{dQ}{dV}\right\}\right] \tag{33}$$

The quantities within the braces can be identified as

$$\frac{-d}{dV}\left[\frac{1}{V\mu}\right] \text{ and } \frac{-d}{dV}\left[\frac{Q}{V\mu}\right], \text{ respectively}$$

Equation (33) is readily integrated to yield

$$C = \frac{H}{\lambda_x}\frac{1}{V\mu} - \frac{\lambda_{\tilde{W}}}{\lambda_x}\frac{Q}{V\mu} + C_1 \tag{34}$$

where C_1 is an arbitrary constant. Hence for the time-range-fuel problem, the solution with altitude-dependence suppressed is

$$\frac{1}{\mu} = \sin\gamma + \left(\frac{H}{\lambda_x V\mu} - \frac{\lambda_{\tilde{W}}}{\lambda_x}\frac{Q}{V\mu} + C_1\right)\cos\gamma \tag{35}$$

To express the above result in the form $\gamma = \gamma(\mu)$, we need to relate the integration constant C_1 to equilibrium values of μ and γ corresponding to unaccelerated flight. Unlike the situation in the simpler problem, the interpretation of Eq. (35) is not straightforward.

From a practical viewpoint the time-range problem is of main interest since minimum-fuel problems with fixed throttle are rare. The fuel-range problem will not be discussed further in the present paper, and in subsequent development the fuel multiplier $\lambda_{\tilde{W}}$ will be taken as zero.

Investigation of equilibrium points with $\lambda_{\tilde{W}} = 0$ results in a plot of the values of H/λ_x vs airspeed as shown in Fig. 4 for a typical parabolic $(T-D)$ distribution. In Fig. 4 three separate regimes can be identified. H/λ_x values to the left of the $(T-D)_{max}$ velocity are positive, while those between the $(T-D)_{max}$ point and the $V(T-D)_{max}$ point have a negative sign. All H/λ_x values to the right of the speed for $V(T-D)_{max}$ are positve. Any of these values may be used to evaluate the arbitrary constant C_1 as follows. As in Eq. (25)

$$\tilde{\mu} = \sin\tilde{\gamma} \tag{36}$$

$$\tilde{V} = V|_{\text{Equilibrium value of } \frac{H}{\lambda_x}} \tag{37}$$

$$C_1 = \cot\tilde{\gamma} - \frac{H}{\lambda_x}\frac{1}{\tilde{V}\tilde{\mu}} \tag{38}$$

Using (38) in (35) putting

$$\Delta = \left[\frac{H}{\lambda_x}\left\{\frac{1}{V\mu} - \frac{1}{\tilde{V}\tilde{\mu}}\right\} + \cot\tilde{\gamma}\right]$$

and using a well-known trigonometric identity.

$$\gamma = \tan^{-1}\left[\frac{1}{\Delta}\right] + \cos^{-1}\left[\frac{1}{\mu\sqrt{\Delta^2+1}}\right] \tag{39}$$

Equation (39) is the Euler solution to the time-range problem with altitude dependence of μ suppressed. This solution was evaluated for representative H/λ_x values from each of the three equilibrium regimes in Fig. 4. It is then found that H/λ_x values in the first and second equilibrium regimes produce oscillatory Euler solutions, similar to those given in Fig. 3. The solutions in Fig. 5 were obtained using an H/λ_x value from the third equilibrium regime and bear some resemblance to those in Fig. 2.

In summary, the range problem has oscillatory solutions when a positive margin of thrust over drag exists. With zero thrust, the solution obtained is the flattest glide with a family of transients to and from the maximum lift-to-drag point. For the time-range problem, values of H/λ_x to the left (low-speed end) of the $V(T-D)_{max}$ point produce oscillatory solutions while, on the right of the $V(T-D)_{max}$ point, a family of transients to and from the equilibrium point defined by the choice of H/λ_x is obtained.

Legendre-Clebsch Necessary Condition

From the Euler-Lagrange equations, with $\lambda_{\tilde{W}} = 0$

$$\frac{\partial H}{\partial\gamma} = -\lambda_V g\cos\gamma + \lambda_h V\cos\gamma - \lambda_x V\sin\gamma \tag{40}$$

and

$$\frac{\partial^2 H}{\partial\gamma^2} = (\lambda_V g - \lambda_h V)\sin\gamma - \lambda_x V\cos\gamma \tag{41}$$

Setting the left side of Eq. (40) to zero as required for a stationary minimum of H leads to

$$\sin\gamma = \frac{(\lambda_h V - \lambda_V g)\sigma}{\sqrt{(\lambda_h V - \lambda_V g)^2 + \lambda_x^2 V^2}} \tag{42}$$

and

$$\cos\gamma = \frac{\lambda_x V \sigma}{\sqrt{(\lambda_h V - \lambda_V g)^2 + \lambda_x^2 V^2}} \tag{43}$$

where $\sigma = \pm 1$. Using Eqs. (42) and (43) in Eq. (41), it is possible to determine σ.

Next, the transversality conditions for the range problem may be employed. These lead to

$$\lambda_x = 1, \quad \frac{\partial^2 H}{\partial \gamma^2} > 0 \quad \text{if } \gamma \text{ lies in the second or third quadrant} \tag{44}$$

$$\lambda_x = -1, \quad \frac{\partial^2 H}{\partial \gamma^2} < 0 \quad \text{if } \gamma \text{ lies in the first or fourth quadrant} \tag{45}$$

viz., $\lambda_x = 1$ for range minimization and $\lambda_x = -1$ for range maximization.

From Eq. (44) it is clear that with no restrictions on path-angle γ, the minimum-range-climb trajectory is that which maximizes the range in the negative direction, a result which is perhaps obvious. The implication is that with no constraint on the final value of time or fuel, the "steepest-climb" problem does not possess a minimum or even a lower bound.

Attention is drawn to the solution to this problem given by Miele[8] using the Green's theorem device. According to Ref. 8, the optimal trajectory for the "steepest climb" problem consists of a central path flown along the $(T-D)_{\max}$ locus in the airspeed-altitude chart with vertical climb/dive transitions at the ends to meet the boundary conditions, if they are off the $(T-D)_{\max}$ path. There is an important difference in vehicle modeling from that of the present work which should be noted as a key to resolving the emerging disparties in character of optimal paths. The analysis of Ref. 8 in essence replaces $\cos\gamma$ in Eq. (3) with unity so that the problem solved is maximum altitude in a given distance (arc length) rather than in a given range.

Consider, next, the imposition of limits on path-angle γ, say $-90 \le \gamma \le 90$ deg. In this case, since final time is unspecified, it is clear that by alternating between vertical-climb and vertical-dive paths, the range-to-climb can be made identically zero. This is a consequence of the intermediate vehicle modeling in which there is no limit to the path-angle rate.

It is of interest to examine vertical-flight sequences comprised of alternating up and down segments. Consider, for example, the case in which specified initial and final altitudes and velocities call for a net increase in specific energy. An initial vertical-flight transition, either up or down as appropriate, is performed to the neighborhood of the maximum of specific excess power (speed $\tilde{V}$ in Fig. 6). Choosing a pair of reversal airspeeds V^* (below $\tilde{V}$) and V^{**} (above $\tilde{V}$), an alternating sequence of straight-up and straight-down trajectory segments is constructed. In the case of net energy gain, both V^* and V^{**} should correspond to positive $\dot{E} = V(T-D)/W$. The relative duration of the segments can be adjusted so that the time-averaged speed is $\tilde{V}$. If V^* and V^{**} are chosen sufficiently close to $\tilde{V}$, the average energy rate can be made as close to the maximum value as one wishes. The motion during this alternating sequence is vertical and net-straight-up as long as the energy rates at V^* and V^{**} are positive. The limiting case of chattering at $\tilde{V}$ corresponds to minimum time as an auxiliary performance index, the primary one, "steepness," being independent of the parameters of the sequence. A final transient, straight up or straight down, is flown to meet the final specifications on speed and altitude. In the case of net energy loss specified, speeds V^* and V^{**} with negative energy rates should be chosen for the rectangular-wave construction of the path-angle history.

Returning to the maximum-range problem, it should be noted that the Legendre-Clebsch necessary condition is met in strengthened form for values of the path angle γ in the first or fourth quadrants. However, physical reasoning makes it clear that a range-maximization problem without time or fuel constraints will not possess a proper maximum, or even an upper bound. In view of the above, the problem of interest is to maximize the range of climb from an inital (V,h) pair to a final (V,h) pair in a fixed time. This problem is of value in studies of the type reported in Ref. 9 for a point-mass-modelled vehicle.

It may be noted that in the cases of time and/or fuel minimization problems with range open, the Legendre-Clebsch necessary condition is met only in weak form along central arcs, and, hence, these trajectories fall into the class of singular extremals.

Conjugate-Point Test

The Legendre-Clebsch necessary condition is met with a margin for the time-range problem, and hence the Euler solution (17) with $\lambda_{\tilde{W}} = 0$ furnishes a relative minimum for intial and terminal points sufficiently close together. For extremals of finite length, however, the task of ensuring that the second variation is nonnegative for admissible neighboring paths leads to the accessory-minimum problem in the calculus of variations. This, in essence, boils down to a search for a system of admissible variations, not identically zero, which offer the most severe competition in the sense of minimizing the second variation. If a system of nonzero variations can be found which makes the second variation zero, then it is clear that a neighboring path is competitive and that the test extremal furnishes at best an improper minimum and at worst a merely stationary value.[10] The first value of the independent variable $x = x^* > x_0$ for which such a nontrivial system can be found defines a conjugate point.

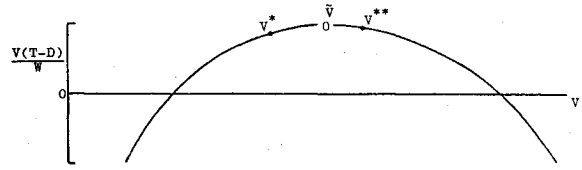

Fig. 6 Parabolic distribution of specific excess power vs airspeed.

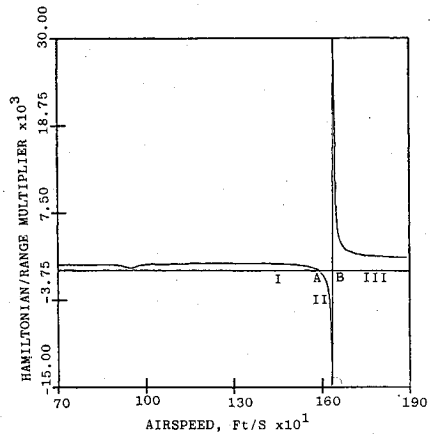

Fig. 7 H/λ_x vs airspeed at constant specific energy for F-4 aircraft for unaccelerted flight.

Following the analysis of Ref. 10 for the Mayer problem, the rank of the matrix of variations of states and the multiplier corresponding to the state being minimized, with respect to the initial values of costates, is evaluated along the test extremal; viz.,

$$\text{the rank of} \begin{bmatrix} \frac{\partial x_2}{\partial \lambda_{1_0}} & \frac{\partial x_2}{\partial \lambda_{2_0}} & \cdots\cdots\cdots & \frac{\partial x_2}{\partial \lambda_{n_0}} \\ \vdots & & & \vdots \\ \frac{\partial x_n}{\partial \lambda_{1_0}} & \frac{\partial x_n}{\partial \lambda_{2_0}} & \cdots\cdots\cdots & \frac{\partial x_n}{\partial \lambda_{n_0}} \\ \frac{\partial \lambda_1}{\partial \lambda_{1_0}} & \frac{\partial \lambda_1}{\partial \lambda_{2_0}} & \cdots\cdots\cdots & \frac{\partial \lambda_1}{\partial \lambda_{n_0}} \end{bmatrix} \tag{46}$$

provides the criterion for the existence of a conjugate point. If the rank of the test matrix (46) drops at any point along the test extremal, it is indicative of the occurrence of a conjugate point.

For the time-range problem, changing the independent variable to range and interpreting H as the time multiplier, the test matrix (46) becomes

$$\begin{bmatrix} \frac{\partial V}{\partial \lambda_{h_0}} & \frac{\partial V}{\partial H_0} & \frac{\partial V}{\partial \gamma_0} \\ \frac{\partial t}{\partial \lambda_{h_0}} & \frac{\partial t}{\partial H_0} & \frac{\partial t}{\partial \gamma_0} \\ \frac{\partial \lambda_h}{\partial \lambda_{h_0}} & \frac{\partial \lambda_h}{\partial H_0} & \frac{\partial \lambda_h}{\partial \gamma_0} \end{bmatrix} = \begin{bmatrix} \frac{\partial V}{\partial \lambda_{h_0}} & \frac{\partial V}{\partial H_0} & \frac{\partial V}{\partial \gamma_0} \\ \frac{\partial t}{\partial \lambda_{h_0}} & \frac{\partial t}{\partial H_0} & \frac{\partial t}{\partial \gamma_0} \\ 1 & 0 & 0 \end{bmatrix} \tag{47}$$

Note that time appears in this problem as a state-like variable with

$$t' = \frac{1}{V\cos\gamma} \tag{48}$$

A prime on the variables denotes differentiation with respect to the range variable x.

From Eq. (47), the sign of

$$\frac{\partial V}{\partial \gamma_0}\cdot\frac{\partial t}{\partial H_0} - \frac{\partial V}{\partial H_0}\cdot\frac{\partial t}{\partial \gamma_0} \tag{49}$$

evaluated along the Euler solution determines the rank of the matrix (47). If the sign changes at any point on the time-range trajectory, it is indicative of a conjugate point.

The Euler solution obtained for the time-range problem with altitude dependence of μ suppressed, may now be tested for conjugate points. In view of the particularly simple form of the conjugate-point test for this problem, it seems reasonable to attempt to obtain analytical approximations for the partial derivatives in Eq. (49).

Linearizing the equations of motion and the Euler equation (17) with range as the independent variable about an equilibrium point at a particular altitude, one obtains

$$\delta V' = a_0\delta V - a_1\delta\gamma \tag{50}$$

$$\delta t' = -a_2\delta V + a_3\delta\gamma \tag{51}$$

$$\delta\gamma' = a_4\delta V - a_5\delta\gamma + a_6\delta H \tag{52}$$

where

$$a_0 = \frac{g}{WV\cos\gamma}\frac{\partial (T-D)}{\partial V} \tag{53}$$

$$a_1 = \frac{g}{V} \tag{54}$$

$$a_2 = \frac{1}{V^2\cos\gamma} \tag{55}$$

$$a_3 = \frac{\sin\gamma}{V\cos^2\gamma}$$

$$a_4 = -\frac{\cos\gamma}{V^4}\frac{g}{\lambda_x}\frac{H}{\lambda_x} + \frac{\partial (T-D)}{\partial V}\frac{g}{V^2(T-D)}\left[1-\frac{\cos\gamma}{V}\frac{H}{\lambda_x}\right] + \frac{g}{V(T-D)^2}\left\{\frac{\partial (T-D)}{\partial V}\right\}^2\left[1-\frac{\cos\gamma}{V}\frac{H}{\lambda_x}\right] + \frac{g}{V(T-D)}\frac{\partial^2 (T-D)}{\partial V^2}\left[\frac{\cos\gamma}{V}\frac{H}{\lambda_x}-1\right] \tag{56}$$

$$a_5 = a_0 \tag{57}$$

$$a_6 = \frac{\cos\gamma}{V^3(T-D)}\frac{g}{\lambda_x}\left[V\frac{\partial (T-D)}{\partial V} + (T-D)\right] \tag{58}$$

Equations (50-52) constitute a linear, constant-coefficient system which can be solved using Laplace transforms. (Initial conditions on δV and δt are zero.) Putting

$$\omega_n^2 = (a_1a_4 - a_0a_5) \tag{59}$$

and

$$T = \frac{-a_3}{a_0a_3 - a_1a_2} \tag{60}$$

and canceling out common constants in the numerator, it can be shown that

$$\frac{\partial V}{\partial \gamma_0}\cdot\frac{\partial t}{\partial H_0} - \frac{\partial V}{\partial H_0}\cdot\frac{\partial t}{\partial \gamma_0} \doteq \frac{\delta V(x)}{\partial \gamma_0} L^{-1}\left[\frac{\omega_n^2}{s^2(s^2+\omega_n^2)}\right] - \left\{\frac{\delta V(x)}{\delta H_0}\right\}^2 \tag{61}$$

If ω_n^2 is positive, the roots of the denominator polynomial are complex conjugates and

$$\frac{\partial V}{\partial \gamma_0}\cdot\frac{\partial t}{\partial H_0} - \frac{\partial V}{\partial H_0}\frac{\partial t}{\partial \gamma_0} \doteq \omega_n x\sin(\omega_n x) + 2\cos(\omega_n x) - 2 \tag{62}$$

The right side of Eq. (62), after being zero at $x=0$, will subsequently become zero at

$$x = \frac{2\pi}{\omega_n} \tag{63}$$

implying that conjugate points will occur every full cycle of the oscillatory solution. Hence, if the equilibrium point for the given H/λ_x is stable, i.e., it produces an oscillatory solution, a conjugate point will occur at the end of one full cycle of the oscillation. On the other hand, if ω_n^2 is negative, the roots are real and distinct, symmetric about the imaginary axis. In this case

$$\frac{\partial V}{\partial \gamma_0}\cdot\frac{\partial t}{\partial H_0} - \frac{\partial V}{\partial H_0}\frac{\partial t}{\partial \gamma_0} \doteq -x\cdot d\cdot\sinh(dx) + 2\cosh(dx) - 2 \tag{64}$$

where

$$d = \sqrt{|\omega_n^2|}$$

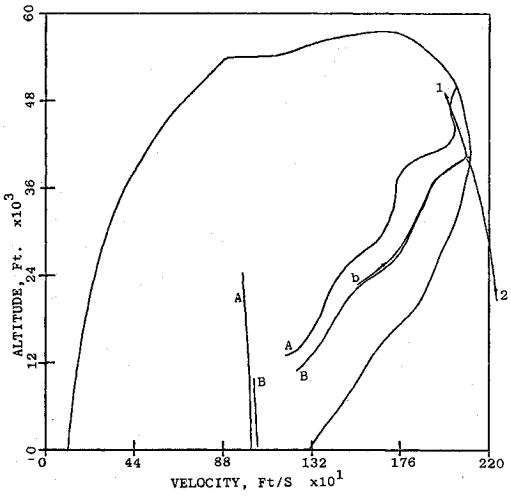

Fig. 8 Flight envelope, energy climb schedule, equilibrium locus and a climb-dash Euler solution; A) energy climb schedule; B) equilibrium locus; C) climb-dash Euler solution.

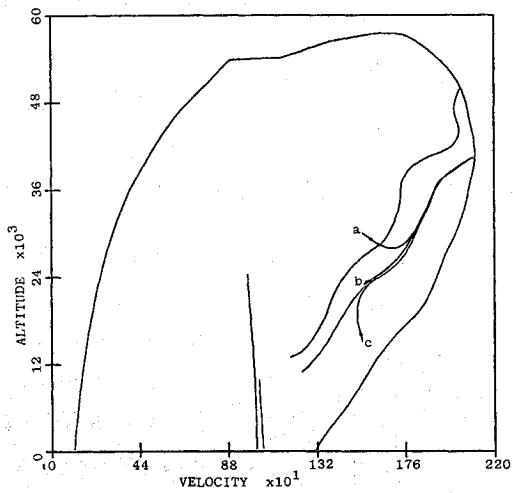

Fig. 9 Euler solutions for the climb-dash problem; a,b,c: Euler solutions.

Expression (64) is zero only at $x=0$. In this case, conjugate points do not occur. From expression (64), then, if the equilibrium point for the given H/λ_x is *unstable,* conjugate points will *not* occur.

The conjugate-point test is now applied to the three regimes of H/λ_x described earlier. As expected, for all values of H/λ_x to the left of the $V(T-D)_{\max}$ point, conjugate points occur, indicating that the Euler solutions obtained with these values of H/λ_x do not afford a maximum to the time-range problem over long intervals. Euler solutions obtained with H/λ_x to the right of the $V(T-D)_{\max}$ point, on the other hand, satisfy the Legendre-Clebsch necessary condition and Jacobi's necessary condition, and hence are optimal trajectories for the time-range problem.

Numerical Solution of the Time-Range Problem

With the insight gained for the time-range problem with altitude dependence on thrust and drag suppressed, one may embark upon a numerical study of the more general case in which the aerodynamic coefficients are functions of Mach number and the thrust is Mach-altitude dependent. The data for a version of the F-4 aircraft with afterburner operative are used in this study. A cubic-spline representation[11] is used to compute the values of zero-lift drag coefficient and the induced-drag coefficient. The drag coefficient is then computed as

$$C_D = C_{D_0}(M) + K(M)C_L^2$$

where $C_L = W/\frac{1}{2}\rho V^2 S$ and C_{D_0} and K are standard notation.

The drag is then obtained as the usual product of drag coefficient, dynamic pressure and the aircraft wing area. A cubic-spline lattice[11] is used to compute the value of thrust at a given altitude and Mach number. Atmospheric density and speed of sound as functions of altitude are interpolated from standard atmosphere tables using cubic splines. The system differential equations are integrated using a fifth-order Runge-Kutta-Verner method with variable step-size.

A plot of H/λ_x vs airspeed for equilibrium flight conditions corresponding to unaccelerted flight with specific energy, $E=h+v^2/2g$, frozen at 60,000 ft is shown in Fig. 7. The three regimes of H/λ_x identified earlier in this paper can be seen in Fig. 7. Numerical integration of the Euler equations with H/λ_x values picked from each of these regimes indicates that the solutions for H/λ_x values to the left of $V(T-D)_{\max}$ are oscillatory. Numerical solutions using H/λ_x to the right of the $V(T-D)_{\max}$ point (high-speed end) are nonoscillatory and violent in character.

Next, a numerical conjugate-point test is set up based on a scheme suggested by Cicala.[12] In this scheme, the partial derivatives with respect to λ_{i_0} required in the matrix (64) are calculated approximately in terms of difference quotients. Small increments in the initial λ_i are employed in the evaluation of neighboring solutions of the original system of Euler equation. The conjugate-point test was carried out for various values of H/λ_x picked from Fig. 10. It was found, as expected, that only the nonoscillatory trajectories corresponding to H/λ_x values to the right of $V(T-D)_{\max}$ satisfy the no-conjugate-point condition. Oscillatory trajectories indicate the existence of a conjugate point after a cycle of oscillation.

From the foregoing, it is clear that the solutions to the time-range optimal-control problem are nonoscillatory and violently unstable in character. Within the permissible range of H/λ_x, as H/λ_x increases, the Euler solutions approach the energy-climb schedule in the *V-h* plane. Of particular interest in practical applications is that trajectory which terminates at the "dashpoint" on the flight envelope, the maximum-level-flight-speed point. To determine the value of H/λ_x which will accomplish this, a plot of the locus of equilibrium points corresponding to unaccelerated flight at constant energy is made. Once this value of H/λ_x is found, what remains to obtain the optimal trajectory is to determine the initial value of the control variable, γ, for a given set of initial conditiions on altitude and airspeed.

In Fig. 8 the level-flight envelope for the F-4 aircraft is shown along with the energy-climb schedule. The discontinuity in the energy-climb schedule due to the transonic drag rise[13] may be noted. The curve *B* is the locus of equilibrium points at each energy level corresponding to unaccelerated flight with the appropriate H/λ_x. The discontinuity due to transonic drag rise is again visible. An Euler solution for initial values of airspeed and altitude close to the equilibrium locus is also shown. To determine this trajectory, an iteration was undertaken on the initial value of the control variable, γ. With quadruple precision on the IBM-370/158, the initial path angle had to be determined to 13 significant digits. To illustrate the sensitivity of the Euler solution to the initial value of path angle γ, the last digit of γ_0 is pertubed in the positive and negative sense, with trajectories 1 and 2 shown in Fig. 8 resulting.

A few more Euler solutions with initial conditions far removed from the equilibrium locus are shown in Fig. 9.

Discussion and Conclusions

In this paper, optimal flight in the vertical plane with a vehicle model intermediate in complexity between point-mass

and energy models was studied. Flight-path angle takes on the role of control varible in the model and range-open problems feature subarcs of vertial flight and singular subarcs as previously studied.

The minimum-range climb problem, first analysed by Miele using the Green's theorem device, has been found to have no minimum, or even a lower bound. There is an important difference in vehicle modeling from that of the present paper which should be noted as a key to resolving disparities between the character of optimal paths emerging. In the analysis of Miele, $\cos\gamma$ is replaced in the range rate equation with unity so that the problem solved is maximum altitude in a given distance (i.e., arc-length) rather than in a given range. This is a necessity with the linear-integral approach, which can accommodate only problems of dimension two and a very special form of the state equations.

From physical considerations it can be seen that when a positive margin of thrust over drag exists, the maximum-range climb trajectory without time or fuel constraints has neither a proper maximum nor an upper bound. In view of this fact, major attention has been accorded to the time-range problem.

For the special case in which the thrust and drag depend only on airspeed, a plot of the ratio of time and range multipliers for equilibrium, corresponding to unaccelerated flight, revealed the existence of three regimes. Positive values of the multiplier ratio on the low-speed side of the maximum specific excess power point and all negative values were shown to yield oscillatory solutions. Although these meet the Legendre-Clebsch necessary conditions, they fail the conjugate-point test. Euler solutions with the time-range multiplier ratio chosen to the right of the maximum specific excess power point satisfy both Legendre-Clebsch and Jacobi necessary conditions and are nonoscillatory in character.

Numerical solution of the Euler equation and a numerical conjugate-point test for the F-4 aircraft data reinforced the conclusions arrived at in the analytical exercise.

From a practical viewpoint, the time-range trajectories which terminate at the "dash point" on the level flight envelope are of particular interest. The time-range multiplier ratio corresponding to this point is determined using the locus of equilibrium points at each energy level corresponding to unaccelerated flight. With this value of the multiplier ratio, the Euler solution for any altitude-airspeed pair is obtained by iterating on the initial value of flight-path angle.

Euler solutions were obtained for various initial conditions. One observes that these tend to funnel rapidly into a certain corridor in the altitude-airspeed chart, in the vicinity of the equilibrium locus corresponding to unaccelerated flight. This feature of the solution family can be exploited in practical situations to simplify the computation of optimal trajectories.

Acknowledgments

The presently reported research was supported by NASA Langley Research Center, Hampton, Virginia, U.S.A., under grant NAG1-203, Drs. Christopher Gracey and Douglas Price serving as Technical Monitors.

References

[1]Kaiser, F., *Der Steigflug mit Strahlflugzeugen—Teil 1, Bahngeschwindigkeit für besten Steigens,* Versuchsbericht 262-02-L44, Messerschmitt A.G., Augsburg, April 1944. (Translated as Ministry of Supply RTP/TIB, translation GDC/15/148T.)

[2]Lush, K.J., "A Review of the Problem of Choosing a Climb Technique with Proposals for a New Climb Technique for High Performance Aircraft," Aeronautical Research Council Report Memo No. 2557, 1951.

[3]Rutowski, E.S., "Energy Approach to the General Aircraft Performance Problem," *Journal of the Aeronautical Sciences,* Vol. 21, No. 3, March 1954, pp. 187-195.

[4]Kelley, H.J., Cliff, E.M., and Weston, A.R., "Energy State Revisited," AIAA Paper 83-2138, Aug. 1983.

[5]Kelley, H.J., "An Investigation by Variational Methods of Flight Paths for Optimum Performance," Sc. D. Dissertation, New York University, May 1958.

[6]Kamke, E., *Differentialgleichungen, Lösungmethoden und Lösungen, Band 1, Gewöhnliche Differentialgleichungen,* Third Edition, Chelsea Publishing Co., New York, N.Y., 1948.

[7]Boyce, W.E. and Diprima, R.C., *Elementary Differential Equations and Boundary-Value Problems,* Third Edition, John Wiley and Sons, New York, N.Y., 1977.

[8]Miele, A., "General Solutions of Optimal Problems in Nonstationary Flight," NACA TM-1388, Oct. 1955.

[9]Weston, A.R., Cliff, E.M., Kelley, H.J., "On-Board Near-Optimal Climb-Dash Energy Management," *1983 American Control Conference,* San Francisco, Calif., June 22-24, 1983, Session TA7, pp. 534-539.

[10]Kelley, H.J. and Moyer, G.H., "Computational Jacobi-Test Procedure," *JUREMA Worskshop on Current Trends in Control,* Dubrovnik, Yugoslavia, June 1984.

[11]Mummolo, R. and Lefton, L., "Cubic Splines and Cubic-Spline Lattices for Digital Computation," Analytical Mechanics Associates, Inc., Rept. No. 72-28, July 1972, Revision dated Dec. 1974.

[12]Cicala, P., *An Engineering Approach to Calculus of Variations,* Levrotto-Bella, Torino, Italy, 1957.

[13]Weston, A.R., Cliff, E.M. and Kelley, H.J., "Altitude Transitions in Energy Climbs," *Automatica,* Vol. 19, No. 2, March 1983, pp. 199-202.

[14]Miele, A., "Problemi di Minimo Tempo nel Volo Nonstazionario degli Aeroplani," *Atti della Academia delle Scienze di Torino,* Vol. 85, 1950-51, pp. 41-42.

[15]Mancill, J.D., "Identical Non-Regular Problems in the Calculus of Variations," *Mathematica y Fisica Teorica,* (Universidad Nacional del Tucumán, República Argentina), Vol. 7, No. 2, June 1950, pp. 130-139.